Direct Electrochemical Preparation of Nanostructured Silicon Carbide and Its Nitridation Behavior

D. Sri Maha Vishnu,[1,2,z] Jagadeesh Sure,[1,2] Hyun-Kyung Kim,[1] Ji-Young Kim,[3] R. Vasant Kumar,[1] and Carsten Schwandt[1,2,*]

[1]*Department of Materials Science and Metallurgy, University of Cambridge, Cambridge CB3 0FS, United Kingdom*
[2]*Department of Materials Science and Metallurgy, University of Nizwa, 616 Nizwa, Sultanate of Oman*
[3]*Advanced Analysis Center, Korea Institute of Science and Technology, Seoul 02792, Korea*

Silicon carbide was synthesized from mixtures of SiO_2 and graphite by applying the concept of the FFC-Cambridge process and several fundamental aspects of the synthesis route were investigated. Porous disks composed of powders of SiO_2 and graphite in molar ratios of 1:0.5, 1:1 and 1:1.5 were prepared by sintering in inert atmosphere and subjected to electro-deoxidation in molten $CaCl_2$ at 1173 K under a range of experimental conditions. Disks of molar ratio 1:1.5, reduced at an applied voltage of 2.8 V for a duration of 6 h, yielded exclusively phase-pure SiC of nanowire morphology as the reaction product, while the other precursor compositions provided significant amounts of calcium silicides. Voltages lower than 2.8 V gave mixtures of SiC with elemental Si and graphite, and voltages higher than that gave CaSi alone. Shorter electro-deoxidation times led to incomplete reduction and allowed for the identification of $CaSiO_3$ as a transient phase. Based on the experimental results a multipath reaction mechanism is proposed, consisting of the electrochemical reduction of SiO_2 and $CaSiO_3$ to Si and the subsequent in-situ carbonization of the Si formed to SiC. The effect of N_2 at high temperature on the electrochemically synthesized SiC was investigated and the formation of nanowire Si_2N_2O was observed. Overall, the process presented is a facile single-step and low-temperature method for the synthesis of SiC with possible commercial prospects.
 [DOI: 10.1149/2.0591814jes]

Manuscript submitted August 20, 2018; revised manuscript received October 15, 2018. Published October 30, 2018.

Silicon carbide is an important non-oxide ceramic material because of its desirable properties, such as high melting point, high hardness and strength, and excellent wear resistance and chemical inertness.[1] SiC has a relatively low density, of 3.21 g/cm^3, compared with other refractory metal carbides, and it is a wide-bandgap semiconductor.[1] Due to this superior blend of thermal, mechanical, chemical and electrical properties, SiC finds diverse applications, as heating elements, as components in automobile brakes and clutches, as ceramic plates in bulletproof vests, as an abrasive, and in electronic devices. SiC is also used as an additive in a variety of composite materials. A more recent research focus has been on nanostructured SiC because of its attractive applications in electrical and energy devices and as a support material for catalysts.[2]

SiC is commercially synthesized by carbothermic reduction of SiO_2 at very high temperature. The commonly used method is the Acheson process in which silica sand is reacted with petroleum coke at above 2773 K in a graphite electric resistance furnace.[1,3] The method is laborious and energy intensive and yields a bulky material with relatively low surface area and many impurities.[1] SiC can also be prepared by various alternative routes. Some of these are gas-phase reactions at high temperature, for instance, the decomposition of organosilicon compounds such as methyltrichlorosilane (CH_3SiCl_3) in the presence of H_2,[4] the reaction of $SiCl_4$ and CCl_4 in the presence of H_2,[5] and the reduction-carburization from Si powder and CCl_4 with Na as a reductant.[6] Further methods are mechanical alloying, liquid phase sintering, arc melting, and sol-gel precipitation.[1] However, all these methods have drawbacks in that they require high energy input, multiple process steps and/or the presence of a substrate.

There is a growing demand for processes that allow the synthesis of metal carbides, particularly SiC, at temperatures lower than those of the conventional production method.[7] The FFC-Cambridge process[8] is a promising approach in this regard. In this, a metal oxide or semimetal oxide serves as the cathode in an electrolytic cell that furthermore contains a molten salt electrolyte of typically $CaCl_2$ and an anode of typically carbon. The cell is then polarized such that the potential of the cathode is negative enough to cause expulsion of oxides ions into the electrolyte, but positive enough to preclude electrolysis of the electrolyte. Many metal oxides and mixtures of metal oxides have been electro-deoxidized in this way to form their parent metals and alloys. The scope and the versatility of the FFC-Cambridge process concerning the oxide precursors used and the metal products made have been reviewed extensively.[9–11]

The FFC-Cambridge process can be modified for the synthesis of metal carbides, by employing a precursor material as the cathode that comprises a mixture of metal oxide and carbon of suitable ratio. Under such conditions, the metal released from its oxide under the influence of the cathodic potential reacts in-situ with the carbon present in the cathode to form the respective metal carbide. Various carbides have been made like this, including TiC,[12,13] ZrC,[14,13] HfC,[15,13] Cr_3C_2,[16] Cr_7C_3,[17] NbC,[18,13] TaC,[13] WC,[19] and SiC.[20] For the latter, the electrolytic cell can be represented as follows.

$$(+)\,C\,|CaCl_2|\,SiO_2,\,C\,(-) \qquad [1]$$

The metal carbides made by electro-deoxidation were typically in the form of powders and consisted of particles in the nanometer range. Zou et al. reported the preparation of SiC from SiO_2/C precursors in molten $CaCl_2$ using an yttria-stabilized zirconia solid oxide membrane as the anode thereby avoiding a carbon anode.[21] The same group also reported the formation of SiC nanowires from SiO_2/C via a combined solid-state reduction and dissolution-deposition mechanism[22] and the further processing of these wires into mesoporous structures for use in supercapacitors.[23]

Despite the earlier reports there are still many uncertainties that prevent the straightforward implementation of the FFC-Cambridge process for the synthesis of SiC at a large scale and with controled morphology. One aspect concerns the optimum precursor composition. This is because it has been found in general that the carbon content of the oxide/carbon precursor has to be higher than the quantity required stoichiometrically due to loss of carbon during processing,[14,15,17,18] although Zhao et al.[20] and Zou et al.[21] have reported that SiC could be made from SiO_2/C of molar ratio 1:1. Another issue concerns the electrochemical process parameters. This is because the main and the side reactions are sensitive to the cathodic potential applied.

The intended cathodic reaction is the electro-deoxidation of SiO_2 to Si followed by the immediate in-situ reaction of the Si with the carbon in the cathode to yield SiC. The reactions read as follows, with the standard electrode potentials calculated from thermodynamic data,[24]

*Electrochemical Society Member.
[z]E-mail: smvd2@cam.ac.uk; vishnu@unizwa.edu.om

depending on whether they are written in one step,

$$SiO_2 + 4\,e^- + C = SiC + 2O^{2-}$$
$$E^0{}_{1173\,K} = 0.999\,V \text{ vs. } Ca/Ca^{2+} \quad [2]$$

or in two steps,

$$SiO_2 + 4\,e^- \rightarrow Si + 2\,O^{2-}$$
$$E^0{}_{1173\,K} = 0.837\,V \text{ vs. } Ca/Ca^{2+} \quad [3]$$

$$Si + C \rightarrow SiC \quad [4]$$

The undesired cathodic reactions are characterized by the involvement of calcium from the electrolyte. These include the deposition of Ca, the in-situ reaction of Ca^{2+} ions with SiO_2 to calcium silicides such as CaSi and Ca_2Si, and the in-situ reaction of Ca^{2+} ions with C to calcium carbide CaC_2.

$$Ca^{2+} + 2\,e^- \rightarrow Ca \qquad E^0{}_{1173\,K} = 0\,V \text{ vs. } Ca/Ca^{2+} \quad [5]$$

$$SiO_2 + Ca^{2+} + 6\,e^- \rightarrow CaSi + 2\,O^{2-}$$
$$E^0{}_{1173\,K} = 0.783\,V \text{ vs. } Ca/Ca^{2+} \quad [6]$$

$$SiO_2 + 2\,Ca^{2+} + 8\,e^- \rightarrow Ca_2Si + 2\,O^{2-}$$
$$E^0{}_{1173\,K} = 0.651\,V \text{ vs. } Ca/Ca^{2+} \quad [7]$$

$$Ca^{2+} + 2\,e^- + 2\,C \rightarrow CaC_2$$
$$E^0{}_{1173\,K} = 0.470\,V \text{ vs. } Ca/Ca^{2+} \quad [8]$$

If the Si formed by electro-deoxidation does not immediately react further to SiC but is temporarily available for other reactions, the following two reactions may occur too.

$$Si + Ca^{2+} + 2\,e^- \rightarrow CaSi$$
$$E^0{}_{1173\,K} = 0.673\,V \text{ vs. } Ca/Ca^{2+} \quad [9]$$

$$Si + 2\,Ca^{2+} + 4\,e^- \rightarrow Ca_2Si$$
$$E^0{}_{1173\,K} = 0.464\,V \text{ vs. } Ca/Ca^{2+} \quad [10]$$

In view of the above, Ca^{2+} discharge on a SiO_2-containing cathode will take place at potentials far less negative to that on an inert cathode such as W or Mo. Qualitatively this has already been demonstrated by Jin et al.[25] and Xiao et al.[26] in cyclic voltammetric studies on the electro-deoxidation of pure SiO_2, although there is only vague information about the precise voltages at which such reactions dominate. Ca^{2+} discharge on a C-containing cathode is also thermodynamically possible at potentials less negative than that on an inert cathode. This has been confirmed experimentally by Fan et al.[13] and Peng et al.,[27] while it has been claimed by Dai et al.[14] that graphite does not react cathodically with Ca^{2+}. Fig. 1 illustrates schematically the competing reactions that are possible under cathodic polarization of SiO_2/C samples in a $CaCl_2$ melt.

Si_3N_4-bonded SiC composites are of considerable interest due to their attractive mechanical and thermal properties.[28] Si_3N_4 is conventionally produced by nitridation of a mixture of Si and SiC through heating in N_2 gas at temperatures where the nitridation of silicon is thermodynamically favored over the nitridation of SiC.[28]

$$3\,Si\ (s) + 2\,N_2\ (g) = Si_3N_4\ (s)$$
$$\Delta G^0{}_{1473\,K} = -269.642\,kJ/mol \quad [11]$$

$$3\,SiC\ (s) + 2\,N_2\,(g) = Si_3N_4\,(s)\ +\ 3\,C\ (s)$$
$$\Delta G^0{}_{1473\,K} = -89.817\,kJ/mol \quad [12]$$

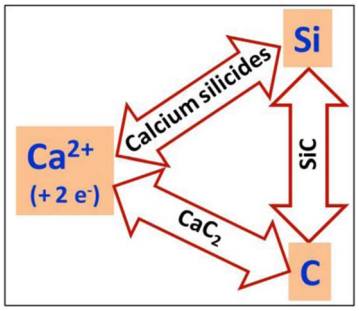

Figure 1. Schematic of competing reactions occurring at a SiO_2/graphite sample under cathodic polarization in $CaCl_2$ melt.

The objective of the current study has been to investigate the electrochemical synthesis of SiC with the aims of optimizing precursor composition, understanding the cathodic reactions, and correlating product morphology with process conditions. A further goal has been to examine the nitridation behavior of the electrochemically prepared SiC and to identify the composition and morphology of the product.

Experimental

Powders of SiO_2 (99% purity, 0.5–5 μm, Sigma Aldrich) and graphite (<20 μm, Sigma Aldrich) were mixed in the molar ratios of 1:0.5, 1:1 and 1:1.5. The mixtures were made into slurries by adding isopropanol together with 1 mass% of polyvinyl alcohol and 0.5 mass% of polyethylene glycol as binder and plasticiser. The slurries were ground in a ball mill and dried at 373 K in air. The process was repeated several times so as to attain a uniform powder mixture. The dry powder was uniaxially pressed into disks of 0.5 g in mass and 13 mm in diameter. The disks were sintered at 1523 K in a stream of Ar with 5 vol% H_2 for 3 h to provide sufficient strength for further processing. The open porosities of the disks were measured by Archimedes' method.

Anhydrous $CaCl_2$ was obtained from $CaCl_2 \cdot 2H_2O$ (Sigma Aldrich) by drying at 423 K in air and then at the same temperature in vacuum for 48 h. The dried $CaCl_2$ was loaded into an alumina crucible that was placed inside a gastight Inconel retort with provision for the insertion of electrodes from the top. The retort was brought to the operating temperature of 1173 K and constantly flushed with Ar. The $CaCl_2$ melt was subjected to pre-electrolysis at 2.8 V for several hours, using a Ni coil as the cathode and a high-density graphite rod (Tokai Carbon, UK), degassed at 400 K in vacuum for 12 h, as the anode, until all redox-active impurities had been removed. A sintered SiO_2/graphite disk, tied with Ni wire, was employed as the cathode in the electro-deoxidation, using the same graphite anode as before. A Ni/NiO assembly was used to monitor the potentials of the individual electrodes.[29] The SiO_2/graphite disks were subjected to electro-deoxidation under different experimental conditions, including (i) cathodes of three compositions as detailed above, (ii) applied voltages of 2.5, 2.8 and 3.1 V, and (iii) process durations of 20 min, 3 h and 6 h, all as compiled in Table I. Cyclic voltammetry was carried out with a W wire as an inert working electrode and with a graphite rod as a reactive working electrode. All potentials were quoted with respect to the Ca/Ca^{2+} potential. This was identified by extrapolating the linear region of the cathodic branch to zero current, thus eliminating any ambiguity originating from the gradual increase of the current prior to Ca deposition due to electronic conduction through the polarized melt.[30]

After completion of each experiment, the electrodes were lifted above the melt and cooled to room temperature. The products were thoroughly rinsed with distilled water until free from salt and dried in vacuum at room temperature. The crystallographic phases, microstructures and elemental compositions of the samples before and after electro-deoxidation were identified by X-ray diffraction analysis (XRD) (Philips PW 1830), scanning electron microscopy (SEM) (FEI Nova NanoSem 450) and energy-dispersive X-ray spectroscopy

Table I. Electro-deoxidation experiments of SiO_2/graphite disks carried out in $CaCl_2$ melt at 1173 K under argon.

Experimental conditions			
SiO_2:graphite (in moles)	Voltage and time	Phases formed	Residual oxygen
1:1	2.5 V for 6 h	graphite (M), Si (SH), SiC (m)	16,300 ppm
1:1	2.8 V for 6 h	SiC (M), Si_5C_3, CaSi, Ca_2Si	-
1:1	3.1 V for 6 h	CaSi	-
1:1.5	2.5 V for 6 h	graphite (M), SiC (SH)	81,400 ppm
1:1.5	2.8 V for 6 h	SiC	22,600 ppm
1:1.5	3.1 V for 6 h	CaSi	13.20 %
1:0.5	2.8 V for 6 h	CaSi (M), SiC (SH), Ca_2Si (trace)	-
1:1.5	2.8 V for 20 min	graphite (M), SiO_2 (M), $CaSiO_3$ (SH)	-
1:1.5	2.8 V for 3 h	graphite (M), SiO_2 (M), SiC, $CaCO_3$ (m)	-

M - major, SH - second highest, m - minor.

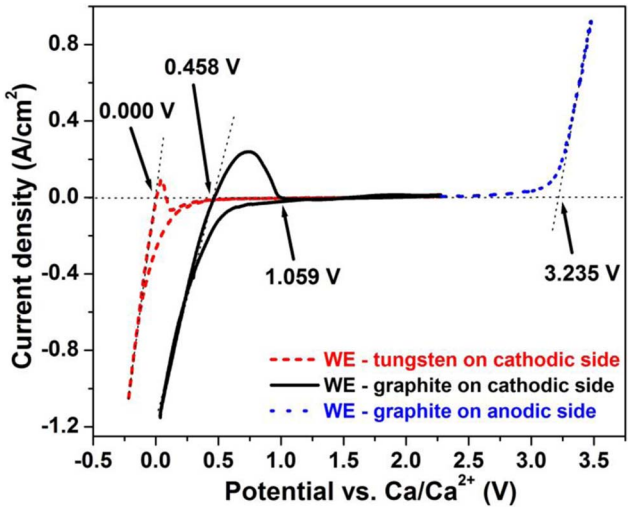

Figure 2. Cyclic voltammograms with W as the working electrode on the cathodic side and with high-density graphite as the working electrode on the cathodic and the anodic sides in $CaCl_2$ melt at 1173 K at a scan rate of 20 mV/s. Graphite rods and Ni coils were used as the counter electrodes in the former and latter cases, respectively. Ni/NiO was used as the reference electrode.

(EDX) (Bruker X Flash 6I100). In selected cases, the reduced samples were further characterized by transmission electron microscopy (TEM) (FEI Tecnai G2-F20). The residual oxygen content of the reduced samples was determined with the hot extraction method (ELTRA ONH 2000).

The effect of N_2 at elevated temperature on the electrochemically prepared SiC was investigated by heating a SiC sample of about 20 mg under a continuous flow of N_2 of 100 mL/min at 1473 K for 8 h, and subsequently studying the phase composition and morphology of the reaction product. The thermokinetic behavior was examined by subjecting a SiC sample of 200 mg to simultaneous thermogravimetric and differential scanning calorimetric analysis (TG/DSC) (SDT Q600, TA Instruments) using a heating rate of 20 K/min from 298 to 1473 K in a stream of N_2.

Results and Discussion

Electrochemical behavior of graphite during cathodic polarization in $CaCl_2$ melt.—Fig. 2 shows cyclic voltammograms recorded in a $CaCl_2$ melt, with a W working electrode on the cathodic side, and with a high-density graphite working electrode on the cathodic and the anodic sides. The reduction of Ca^{2+} on W was found to begin at 0.00 V, which confirmed its inertness. In contrast, appreciable reduction on graphite progressed from +1.059 V onwards. The Ca^{2+} discharge on graphite at potentials less negative to that on W may be attributed to the formation of Ca-C compounds, most likely CaC_2, as expressed in Eq. 8. Based on the present results, graphite has to be considered a reactive electrode when polarized cathodically in a $CaCl_2$ melt. Comparing the linear regions of the cathodic branches of the cyclic voltammograms, the electrochemical window of $CaCl_2$ in the presence of a graphite electrode is lower by ~450 mV than in the presence of an inert electrode.

In line with the observations of the present study, Fan et al.[13] and Peng et al.[27] likewise suggested the formation of CaC_2 from graphite and Ca^{2+} during cathodic polarization in a $CaCl_2$ melt. In contrast, Dai et al.[14] found in cyclic voltammetry studies with a metallic cavity electrode at 1123 K that graphite did not react with Ca^{2+} during cathodic polarization in $CaCl_2$ but behaved more like an inert electrode.

Sintering behavior and microstructure of SiO_2/graphite mixtures.—SiO_2/graphite disks, made from mixtures of the SiO_2 and graphite powders in the molar ratios of 1:0.5, 1:1 and 1:1.5 and sintered at 1523 K in Ar with 5 vol% H_2 for 3 h, possessed open porosities of about 40%. Figs. 3a–3c show the XRD patterns of the SiO_2 and graphite powders along with that of a sintered SiO_2/graphite disk of molar ratio 1:1.5. The peaks at 2θ of 20.95°, 26.73° and 50.20° seen in the XRD patterns for the pure SiO_2 and the sintered SiO_2/graphite mixture originate from the diffractions of the (100), (011) and (112) planes of quartz, and those at 26.5° and 54.6° in the XRD pattern for the pure graphite and the sintered SiO_2/graphite mixture are from the (002) and (004) planes of graphite. The XRD analysis confirms that the starting materials were phase pure and that, in line with thermodynamic expectations, they underwent no reaction during sintering.

Figs. 3d–3i show SEM images and EDX spectra of the SiO_2 and graphite powders. The micrographs reveal that the SiO_2 consisted of particles of irregular morphology with size in the range of 0.15–5 μm, while the graphite consisted of particles of flaky morphology with size in the range of 2–12 μm; and the elemental analysis confirmed that there were no significant impurities. Figs. 4a–4f show SEM images of the cross-sections from the sintered SiO_2/graphite disks of the three different compositions. The two types of particles can be clearly identified by their morphologies and compositions, evidencing that they formed an intimate near-uniform mixture. Elemental maps for Si, O and C of selected regions from the cross-sections are given in Fig. S1 (Supplementary Material).

Electro-deoxidation of SiO_2/graphite mixtures.—*Electro-deoxidation of SiO_2/graphite of molar ratio 1:1 at different voltages.*—SiO_2/graphite disks of molar ratio 1:1 were subjected to electro-deoxidation at applied voltages of 2.5, 2.8 and 3.1 V for durations of 6 h in order to investigate the effect of polarization. The current vs. time curves are shown in Fig. S2. The results of the XRD analysis of the three products are compiled in Table I. At 2.5 V, Si and SiC were observed together with unreacted graphite. At 3.1 V, only CaSi was found. At the intermediate voltage of 2.8 V, SiC was

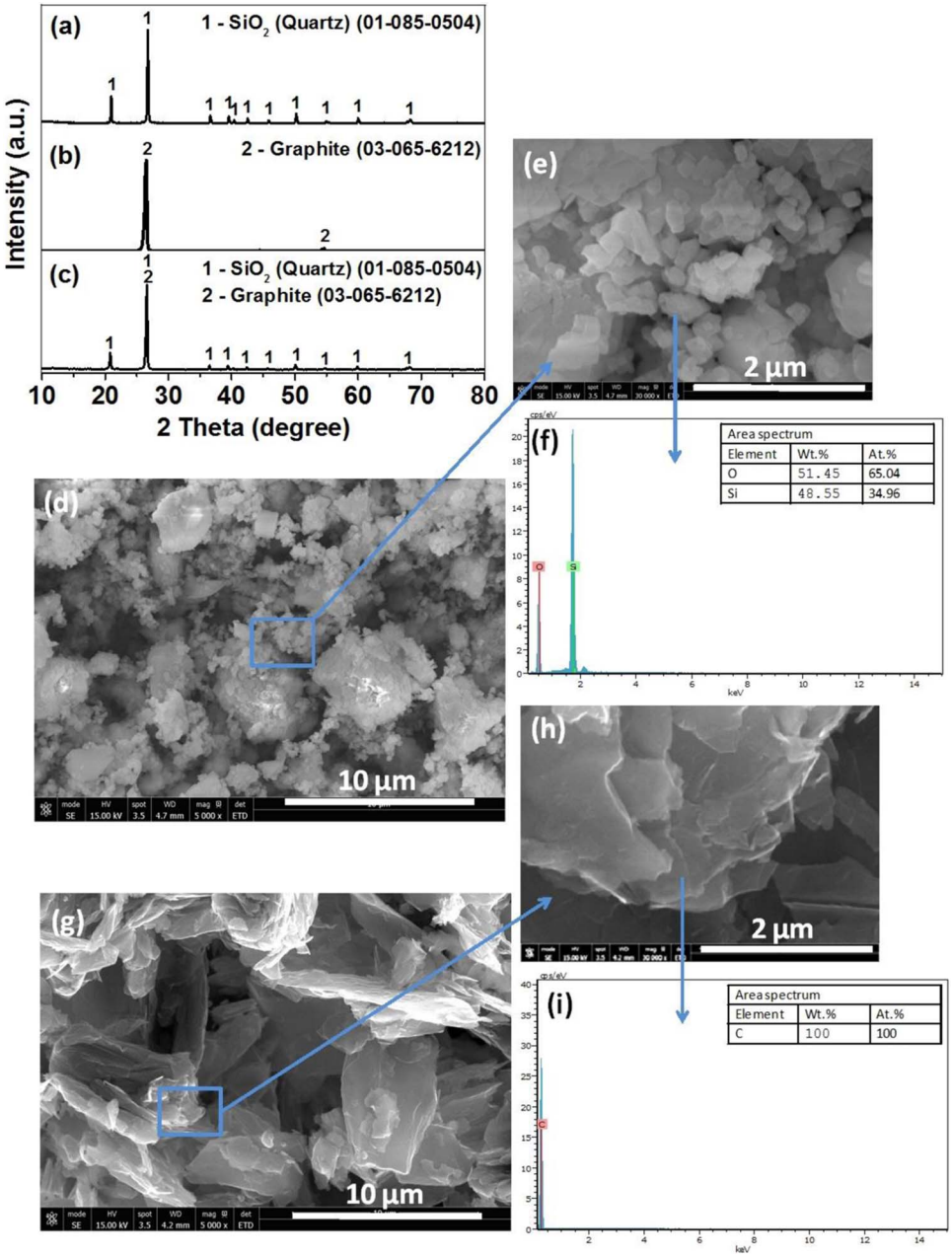

Figure 3. XRD patterns of (a) as-received SiO_2 powder, (b) as-received graphite powder, and (c) SiO_2/graphite disk (molar ratio 1:1.5) sintered at 1523 K in Ar with 5 vol% H_2 for 3 h. (d) SEM image and (e) high-resolution SEM image of SiO_2 powder with (f) corresponding EDX analysis. (g) SEM image and (h) high-resolution SEM image of graphite powder with (i) corresponding EDX analysis.

the major phase, but minor amounts of Si_5C_3, CaSi and Ca_2Si were also present.

The XRD analysis thus demonstrates that, at the low voltage, all SiO_2 was electro-deoxidized, and even though some SiC was formed, its rate of formation was low so that not all graphite was consumed. At the high voltage, undesired reactions involving Ca prevailed. At the intermediate voltage, the complete consumption of the graphite was achieved, but Ca-based by-products were formed. The results therefore indicate that equal quantities of SiO_2 and graphite are insufficient to arrive at a stoichiometric SiC product, presumably because some graphite is lost due to side reactions.

Electro-deoxidation of SiO_2/graphite of molar ratio 1:1.5 at different voltages.—Based upon the above findings, SiO_2/graphite disks of molar ratio 1:1.5 were subjected to electro-deoxidation at applied voltages of 2.5, 2.8 and 3.1 V for durations of 6 h. The current vs. time and cathode potential vs. time curves are shown in Figs. 5a, 5b. In all three cases, the currents initially peaked and then declined toward stable residual values, thus indicating the progression of the cathodic reactions. As expected, the current was higher at higher voltage, while the main characteristics of the curves were similar. The cathode potentials vs. Ca/Ca^{2+} evolved with distinct features that could be directly correlated with the current behavior. The potentials shifted in the more negative direction with increasing reaction time, with stable values reached faster at higher voltage.

The three products obtained after electro-deoxidation were all in the form of powder, as seen from the insets of Fig. 5a. The XRD patterns of the products are shown in Figs. 5c–5e and the phases identified are given in Table I. At 2.5 V, the product was a mixture of SiC and graphite, and at 3.1 V, the product was again pure CaSi. At 2.8 V, however, phase-pure SiC was now obtained. The SiC existed in its cubic β modification, with the peaks at 35.5°, 41.1°, 60.0° and

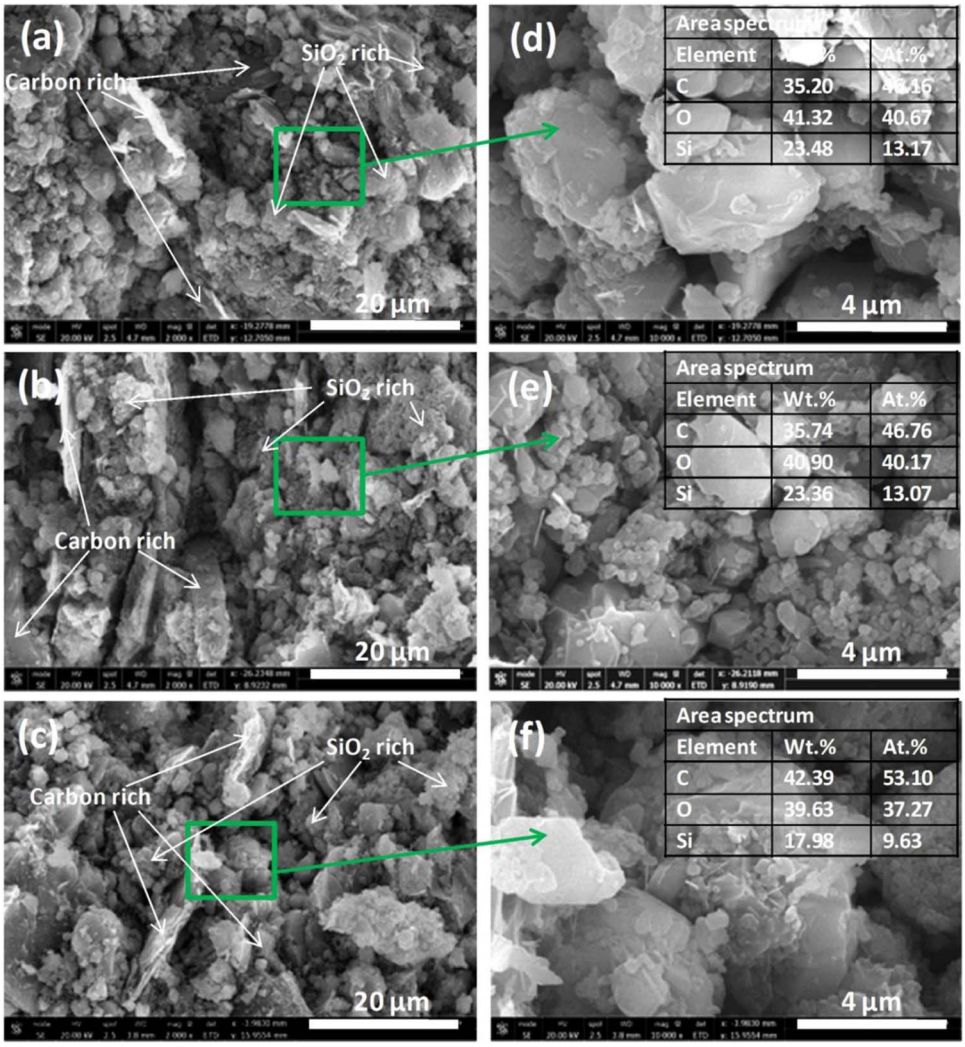

Figure 4. SEM images of cross-sections of SiO_2/graphite disks of molar ratios (a) 1:0.5 (b) 1:1 and (c) 1:1.5, sintered at 1523 K in Ar with 5 vol% H_2 for 3 h, showing SiO_2-rich and graphite-rich regions. (d), (e), (f) High-resolution SEM images with EDX analyses of the indicated areas.

71.6° stemming from the diffractions of its (111), (200), (220) and (311) planes. It has been reported that β-SiC forms preferentially at process temperatures below 1973 K while the α-type prevails at higher temperatures.[31]

Figs. 6a–6f show SEM images of the three products. The microstructure of the product at 2.5 V contained wire-like entities with lengths from a few tens to a few hundreds of nanometers (Figs. 6a, 6d). EDX analysis revealed that they were composed of Si and C, thereby suggesting them to be SiC. In addition, some flaky particles with diameters of a few micrometers were observed that were similar to those in the SiO_2/graphite precursor before processing (Figs. 6a, 6d, Fig. S3). EDX analysis confirmed them to be from carbon, thereby identifying them as unreacted graphite. The microstructure of the product at 3.1 V contained comparatively bulky particles with diameters in the range of several micrometers (Figs. 6c, 6f, Fig. S4). EDX analysis showed them to consist of primarily Ca and Si, thus identifying them as CaSi. Neither SiC nanowires nor graphite flakes were present, and the significant charging during imaging was because of the sample's poor electronic conductivity. Significant levels of O were found (Fig. S5), which were likely due to absorption of and reaction with water in the washing step. The microstructure of the product at 2.8 V was very different (Figs. 6b, 6e), featuring exclusively SiC nanowires. Fig. 7 shows a low-magnification SEM image of the sample, along with the EDX elemental maps for Si and C and a typical EDX analysis. A small quantity of oxygen of about 2.7 mass% was found too. Fig. 8 shows a high-resolution TEM image that clearly indicates the nanoscopic nature of the SiC with good crystallinity and an average particle size of about 20–30 nm. The lattice spacing was measured as approximately 0.25 nm for the SiC (111) plane (inset in Fig. 8) which is coincident with literature values.[21,22]

The occurrence of the different reaction products can be readily understood in view of Eqs. 2 to 8. An applied voltage of about 2.8 V is required to ensure a sufficiently fast formation of the SiC, including the electro-deoxidation of the SiO_2 to Si and its in-situ reaction with the graphite in the cathode. However, at this voltage the formation of CaC_2 through the reaction of the graphite in the cathode with Ca^{2+} ions from the electrolyte is not negligible, and this leads to a partial consumption of the graphite. The arising Si surplus then manifests itself in the formation of Si_5C_3 as a carbon-deficient silicon carbide and of CaSi and Ca_2Si, as seen with the SiO_2/graphite disks of molar ratio 1:1. This notion was further corroborated by electro-deoxidation experiments with SiO_2/graphite disks of molar ratio 1:0.5 under otherwise the same conditions (Fig. S6). In such a cathode, the carbon deficit exists straight from the beginning, and the main compound found in the reduced samples was CaSi (Table I). Consequently, to achieve stoichiometric SiC, a sufficient excess of graphite in the SiO_2/graphite precursor is necessary to compensate for its partial loss as CaC_2. Usefully, CaC_2 reacts with water in the washing step and does not accrue as a by-product in the cathode.

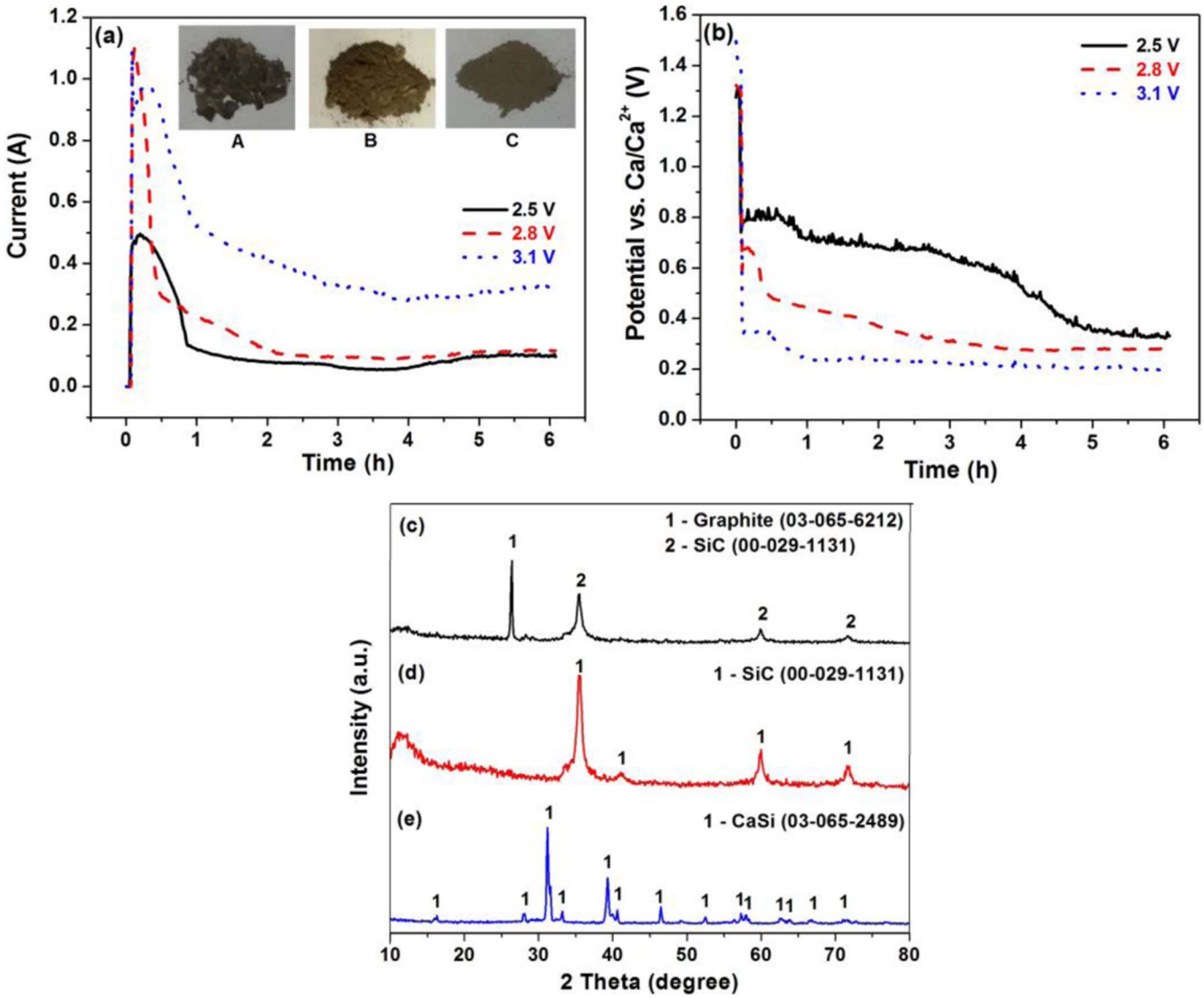

Figure 5. (a) Current vs. time curves and (b) cathodic potential vs. time curves during electro-deoxidation of SiO_2/graphite disks (molar ratio 1:1.5) in $CaCl_2$ melt at 1173 K for 6 h at 2.5, 2.8, and 3.1 V. Insets in (a) show photographs of the three products. (c), (d), (e) XRD patterns of the products obtained at the three different voltages.

The above would also explain the observation of a carbon loss, or the need of a carbon surplus, in related studies. For example, in the preparation of ZrC from ZrO_2, an excess of carbon was required to achieve a phase-pure product,[14] and in the preparation of HfC from HfO_2, a small loss of carbon happened during the process.[15] The effect may be further compounded by the large difference in particle size of the SiO_2 and the graphite in the present case, as this leads to longer diffusion distances in the in-situ reaction of Si with carbon and enhances the possibility of carbon loss via side reactions. For example, in the preparation of Cr_7C_3 from Cr_2O_3, the use of large carbon particles led to a slow rate of carbonization,[17] while in the preparation of NbC from Nb_2O_5, the use of carbon nanoparticles improved the extent of carbonization.[18]

Electro-deoxidation of SiO_2/graphite of molar ratio 1:1.5 for different durations.—In order to investigate the nature of any transient phases occurring in the course of the reduction of SiO_2 in the presence of graphite, partially reduced samples were prepared, by subjecting SiO_2/graphite disks of molar ratio 1:1.5 to electro-deoxidation at an applied voltage of 2.8 V for durations of only 20 min and 3 h. Figs. 9a, 9b show the current vs. time and the cathodic potential vs. time curves from these experiments along with curves from a 6 h run.

The product obtained after 20 min was in the form of a disk, and that after 3 h was a powder, as seen from the insets of Fig. 9a. Figs. 9c, 9d show the XRD patterns of the 20 min and 3 h samples, respectively, and demonstrate that the main transient phase was $CaSiO_3$ and that its amount diminished as the amount of SiC product grew.

Fig. 10a shows a low-resolution SEM image of the cross-section of the sample obtained after 20 min of electro-deoxidation, and Fig. 10b shows SEM image of a smaller area of this cross-section, in which the interface between two separate regions can be clearly discerned. As seen from Figs. 10c, 10d, one region had bulky morphology with particles of SiO_2 and carbon similar to that in the starting material, indicating that practically no reduction had taken place here, while the other region had SiC nanowires together with large particles and flakes, indicating that reduction had commenced but remained incomplete. Separate SEM images of these regions with their dissimilar microstructures are shown in Fig. S7, and an EDX analysis further indicated that the partially reduced regions still had significant quantities of oxygen. Figs. 10e, 10f show the microstructure of the sample

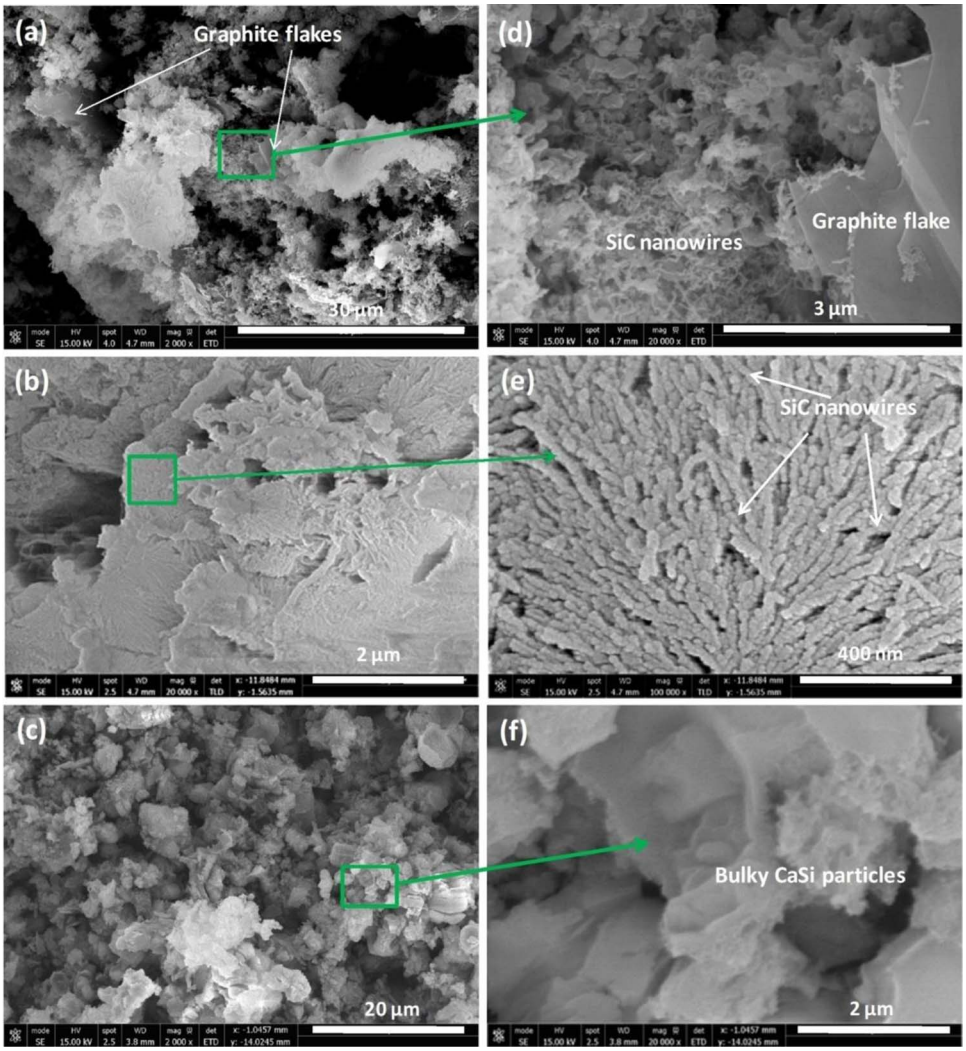

Figure 6. SEM images of the various products obtained from SiO_2/graphite (molar ratio 1:1.5) by electro-deoxidation in $CaCl_2$ melt at 1173 K for 6 h at (a) 2.5 V, (b) 2.8 V, and (c) 3.1 V. (d), (e), (f) High-resolution SEM images of the indicated areas.

obtained after 3 h of electro-deoxidation. The individual particles were identified as SiO_2, graphite and $CaSiO_3$, and the amount of SiC nanowires had increased compared with the shorter experiment. Further SEM images and an EDX analysis are shown in Fig. S8.

Mechanistic considerations.—Ideas about the reaction mechanism of the electro-deoxidation of SiO_2 in the presence of graphite in a $CaCl_2$ melt can be derived from the transient phases, Si and $CaSiO_3$, found in some of the experiments. The following reaction sequences are conceivable.

Direct reduction of SiO_2.—The transient presence of free elemental Si in the cathode, in combination with an amount of SiC, in the experiments at low applied voltage indicates that the electro-deoxidation of SiO_2 directly to Si is one of the reactions occurring. This is then followed by the in-situ reaction of the Si with C to SiC.

$$SiO_2 + 4\,e^- \rightarrow Si + 2\,O^{2-}$$
$$E^0{}_{1173\,K} = 0.837\ V\ vs.\ Ca/Ca^{2+} \qquad [13]$$

$$Si + C \rightarrow SiC \qquad [14]$$

The reduction of SiO_2 to Si, without the temporary formation of other phases, has also been reported to happen in the absence of C.[32] Such direct conversions are likewise known for the reduction of Fe_2O_3[33] and UO_2.[34]

Reduction of SiO_2 via electrochemical formation of $CaSiO_3$.—The transient presence of $CaSiO_3$ in the cathode in the short experiments at intermediate applied voltage may indicate a two-step reduction process, which involves the combined formation of Si and $CaSiO_3$, followed by the electro-deoxidation of the $CaSiO_3$.

$$3\,SiO_2 + 2\,Ca^{2+} + 4\,e^- \rightarrow Si + 2\,CaSiO_3$$
$$E^0{}_{1173\,K} = 1.308\ V\ vs.\ Ca/Ca^{2+} \qquad [15]$$

$$CaSiO_3 + 4\,e^- \rightarrow Ca^{2+} + Si + 3\,O^{2-}$$
$$E^0{}_{1173\,K} = 0.602\ V\ vs.\ Ca/Ca^{2+} \qquad [16]$$

$$Si + C \rightarrow SiC \qquad [17]$$

The reduction of SiO_2 to Si, with the temporary formation of $CaSiO_3$, has indeed been reported when only small amounts of electrolyte were present.[35] Reaction sequences of this kind are also well known from the reduction of TiO_2,[36] Cr_2O_3[30] and Nb_2O_5.[29] It is noted that Ca metallates tend to give very strong peaks in the XRD pattern, so that those of the corresponding metals or suboxides are sometimes obscured.

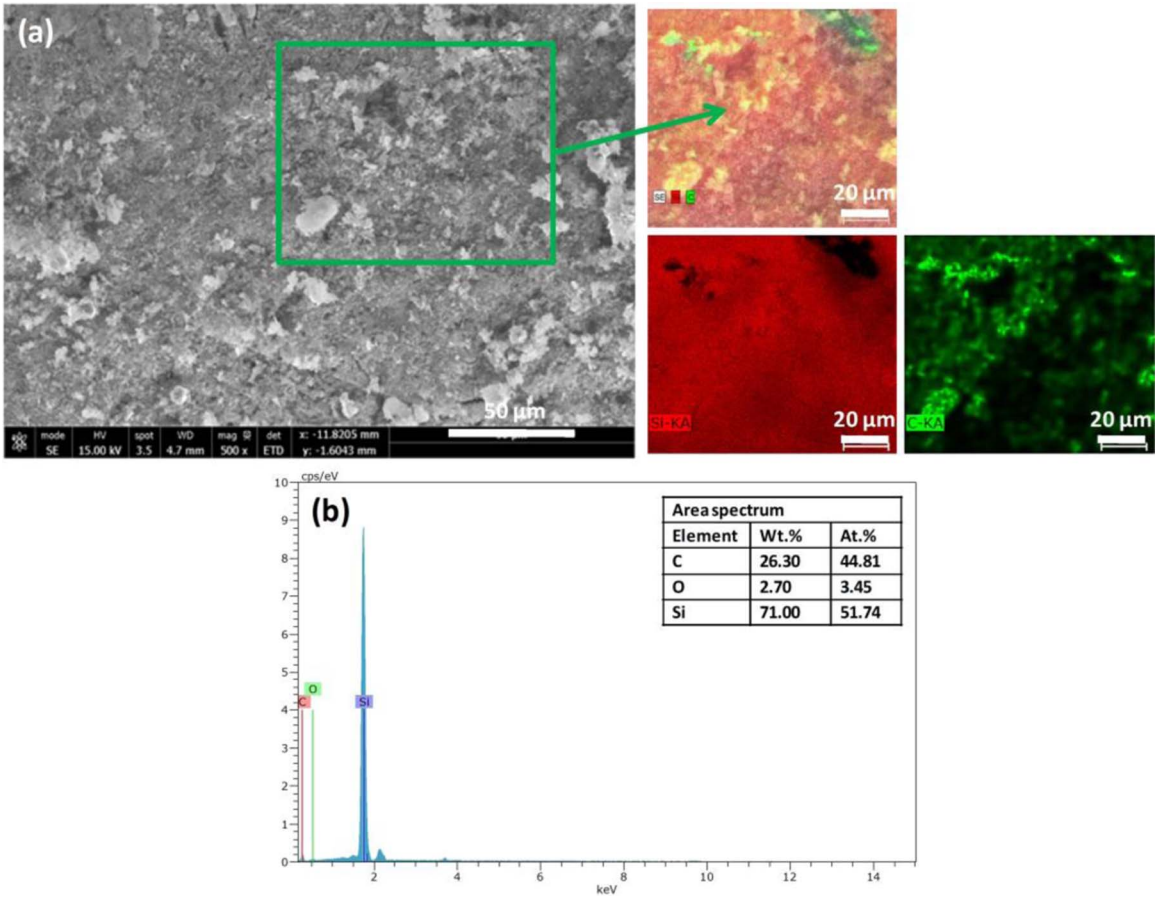

Figure 7. (a) SEM image with EDX elemental maps and (b) EDX spectrum of the SiC product obtained from SiO_2/graphite (molar ratio 1:1.5) by electro-deoxidation in $CaCl_2$ melt at 1173 K for 6 h at 2.8 V.

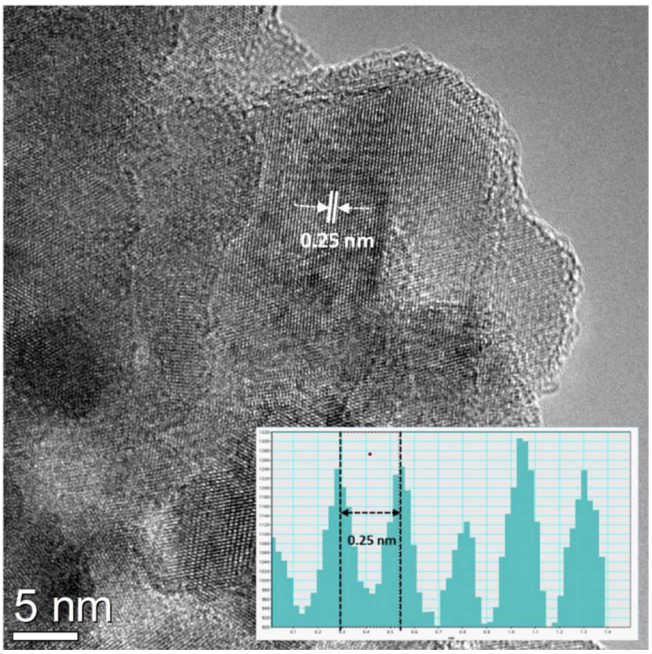

Figure 8. High-resolution TEM image of the SiC product obtained from SiO_2/graphite (molar ratio 1:1.5) by electro-deoxidation in $CaCl_2$ melt at 1173 K for 6 h at 2.8 V. Inset shows the lattice spacing of the (111) plane of SiC.

Reduction of SiO_2 via chemical formation of $CaSiO_3$.—The transient presence of $CaSiO_3$ in the cathode may also be due to its chemical formation from SiO_2 and CaO dissolved in the $CaCl_2$. The CaO originates from insufficient drying of the $CaCl_2$ and forms in the melt during the electro-deoxidation process.

$$SiO_2 + CaO \rightarrow CaSiO_3 \quad [18]$$

$$CaSiO_3 + 4\,e^- \rightarrow Ca^{2+} + Si + 3\,O^{2-}$$
$$E^0{}_{1173\,K} = 0.602\ V\ vs.\ Ca/Ca^{2+} \quad [19]$$

$$Si + C \rightarrow SiC \quad [20]$$

The chemical formation of Ca metallates with CaO from the electrolyte has also been found in the reduction of Ta_2O_5.[37]

Reduction of $CaSiO_3$ via dissolution and deposition.—In the above reaction sequences, the reduction of the $CaSiO_3$ has been written as a solid-state reaction. However, there is significant solubility on the percent level of $CaSiO_3$ in $CaCl_2$ melts with CaO additions.[38] Therefore, it is possible that at least a portion of the $CaSiO_3$ may have entered into the $CaCl_2$ melt during the experiment, from which the Si was then electro-deposited back onto the cathode.

$$CaSiO_3 \rightarrow Ca^{2+} + SiO_3{}^{2-} \quad [21]$$

$$SiO_3{}^{2-} + 4\,e^- \rightarrow Si + 3\,O^{2-}$$
$$E^0{}_{1173\,K} = 0.602\ V\ vs.\ Ca/Ca^{2+} \quad [22]$$

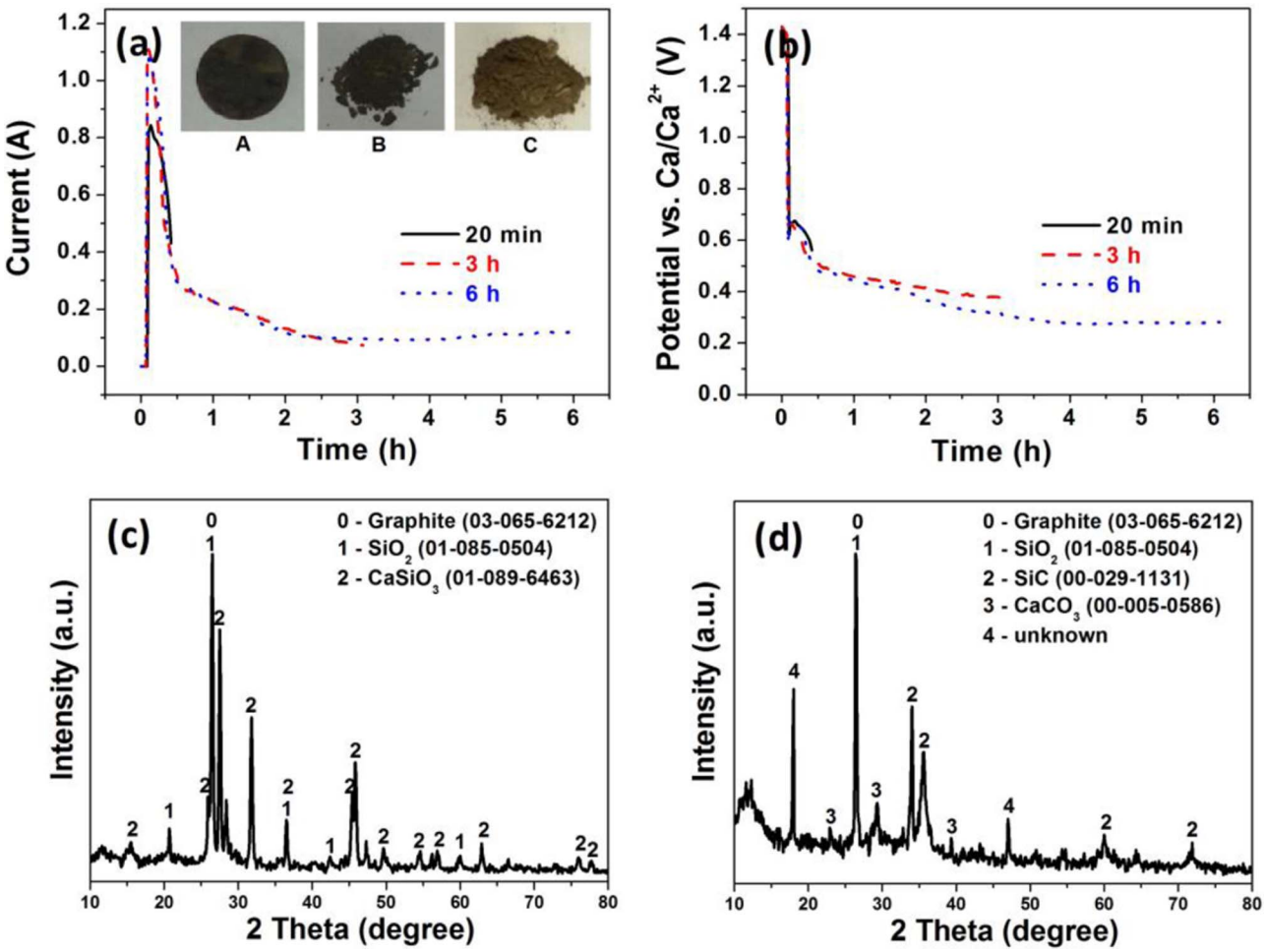

Figure 9. (a) Current vs. time curves and (b) cathodic potential vs. time curves during electro-deoxidation of SiO_2/graphite disks (molar ratio 1:1.5) in $CaCl_2$ melt at 1173 K for 20 min, 3 h and 6 h at 2.8 V. Insets in (a) show photographs of the three products. XRD patterns of the products obtained after (c) 20 min and (d) 3 h.

This type of SiO_2 reduction has been considered to be the dominant one by Xiao et al.[38] and Zou et al.[22]

Overall, the electro-deoxidation of SiO_2 in the presence of graphite in a $CaCl_2$ melt is highly complex and likely to progress via several parallel reaction sequences. These are dependent on the precursor morphology and on the applied voltage and may therefore differ between individual experiments. This highlights the necessity of empirical process optimization as has been done in the present study.

Nitridation of SiC nanowires.—Fig. 11a shows the XRD pattern of the material obtained after heating the electrochemically prepared SiC in N_2 at 1473 K for 8 h. The product contained Si_2N_2O together with the cristobalite phase of SiO_2. Figs. 11b–11d show SEM images and an EDX analysis of the product, notably demonstrating that it had retained its nanowire morphology. The present study is therefore believed to be the first report on the synthesis of nanowire-type Si_2N_2O.

Fig. 11e shows the mass change and heat flow vs. temperature curves recorded in the TG/DSC experiments of the electrochemically made SiC in N_2 atmosphere. The TG curve presents two distinct stages, one involving mass loss (stage I), and one involving mass gain (stage II). The curve begins with a mass loss, which is quite steep from 25 to about 710 K and then becomes rather insignificant. The minimum mass of 99.98% of the original is reached at 870 K. This is followed by a mass gain, which is rather slow up to 1120 K and then becomes quite steep.

Tishchenko et al.[39] studied the thermokinetic behavior of SiC in air by TG/DSC and reported that the mass loss from room temperature to about 467 K was due to the presence of moisture. In line with that, the small endothermic mass loss of the SiC sample up to 475 K may be attributed to the removal of adsorbed moisture. Roy et al.[40] reported that the subsequent oxidation of SiC has two components, active oxidation with oxygen at low activity according to Eq. 23, involving a net mass loss, and passive oxidation with oxygen at high activity according to Eq. 24, involving a net mass gain.

$$\mathrm{SiC} + 2\,\mathrm{O}\ (\text{residual in SiC}) \rightarrow \mathrm{SiO}\ (g) + \mathrm{CO}\ (g) \qquad [23]$$

$$\mathrm{SiC} + 2\,\mathrm{O_2}\ (\text{surrounding gas}) \rightarrow \mathrm{SiO_2}\ (s) + \mathrm{CO_2}\ (g) \qquad [24]$$

Due to the high level of residual oxygen in the electrochemically prepared SiC material (Table I), the mass loss of the SiC up to 870 K may be attributed to active oxidation, with the oxygen evolving in the form of CO and SiO gases.

The endothermic mass gain above 870 K may be ascribed to the reaction of the SiC with N_2. This must involve the formation of Si_2N_2O, as evidenced by the XRD analysis of the nitrided sample. Mechanistically, the formation of Si_2N_2O may include both the residual oxygen

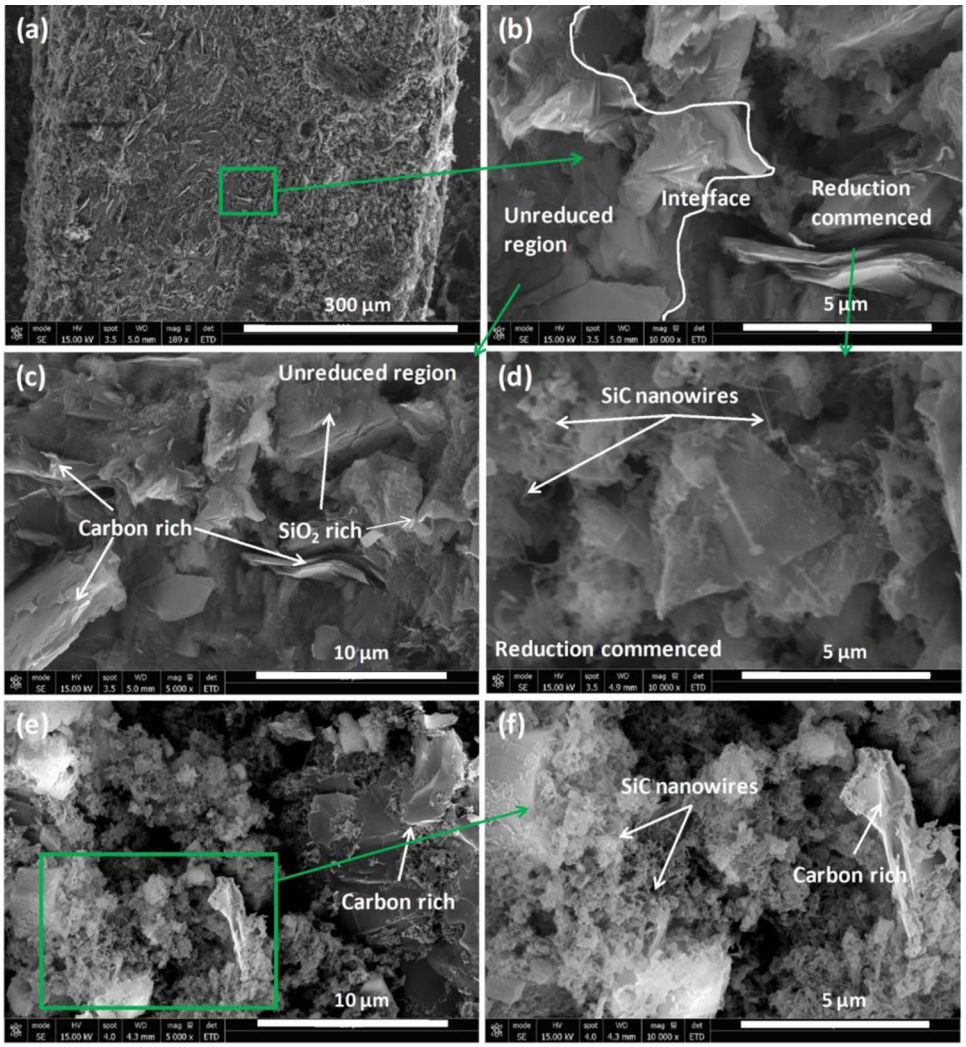

Figure 10. (a) SEM images of the product obtained from SiO_2/graphite (molar ratio 1:1.5) by electro-deoxidation in $CaCl_2$ melt at 1173 K for 20 min at 2.8 V, with (b) enlargement of the indicated area in (a) showing the interface of regions with no reduction and with commencing reduction. High-resolution image of (c) region with no reduction, and (d) region with commencing reduction. (e) SEM images of the product obtained from SiO_2/graphite (molar ratio 1:1.5) by electro-deoxidation in $CaCl_2$ melt at 1173 K for 3 h at 2.8 V, with (f) enlargement of the indicated area in (e).

in the SiC as well as the trace oxygen in the N_2 gas.

$$2\,SiC + CO\,(g) + N_2\,(g) \rightarrow Si_2N_2O + 3\,C$$
$$\Delta G^0{}_{1473\,K} = -109.577\,kJ/mol \qquad [25]$$

$$2\,SiC + {}^1\!/_2\,O_2\,(g) + N_2\,(g) \rightarrow Si_2N_2O + 2\,C$$
$$\Delta G^0{}_{1473\,K} = -351.029\,kJ/mol \qquad [26]$$

Munro and Dapkunas[41] reported that when pure SiC is heated in the presence of pure N_2, it slowly converts into Si_3N_4. They further reported that the additional presence of CO would lead to the formation of oxynitrides. This is in line with the current findings where CO is thought to be released in the active oxidation.

Overall, the observed mass changes and the formation of Si_2N_2O and SiO_2 can be explained by the oxidation and nitridation of the electrochemically made SiC. Some stoichiometric considerations to corroborate this notion are given in the Appendix.

Conclusions

Silicon carbide with nanowire morphology was electrochemically synthesized from SiO_2/graphite mixtures in a $CaCl_2$ melt. Three competing reactions were found to occur in cathodically polarized SiO_2/graphite, (i) the electro-deoxidation of SiO_2 to Si and the subsequent in-situ reaction of the Si with graphite to form SiC, (ii) the reaction of Si with Ca^{2+} ions to form calcium silicides such as CaSi and Ca_2Si, (iii) the reaction of graphite with Ca^{2+} ions to form CaC_2. The successful synthesis of pure SiC requires an optimized combination of the composition of the SiO_2/graphite precursor, the magnitude of the applied voltage, and the duration of the polarization, while deviations from such conditions lead to the incomplete reaction of the Si with the graphite or to the preferential formation of calcium silicide. A significant excess of graphite in the starting material is required to compensate for the loss of carbon through inevitable side reactions. Partially reacted SiO_2/graphite samples contained Si or $CaSiO_3$, which enabled detailed considerations of possible reaction paths.

Nitridation experiments of the electrochemically made SiC at elevated temperature showed the formation of Si_2N_2O. TG/DSC studies with the SiC in N_2 atmosphere indicated distinct stages, attributable to the loss of moisture, the partial oxidation with residual oxygen in the material, and the reaction with N_2.

Notably, the SiC is in its β-phase and has nanowire morphology, and the Si_2N_2O retains this nanowire morphology. This may make possible the application of the materials in the energy and other sectors as will be elaborated in future reports.

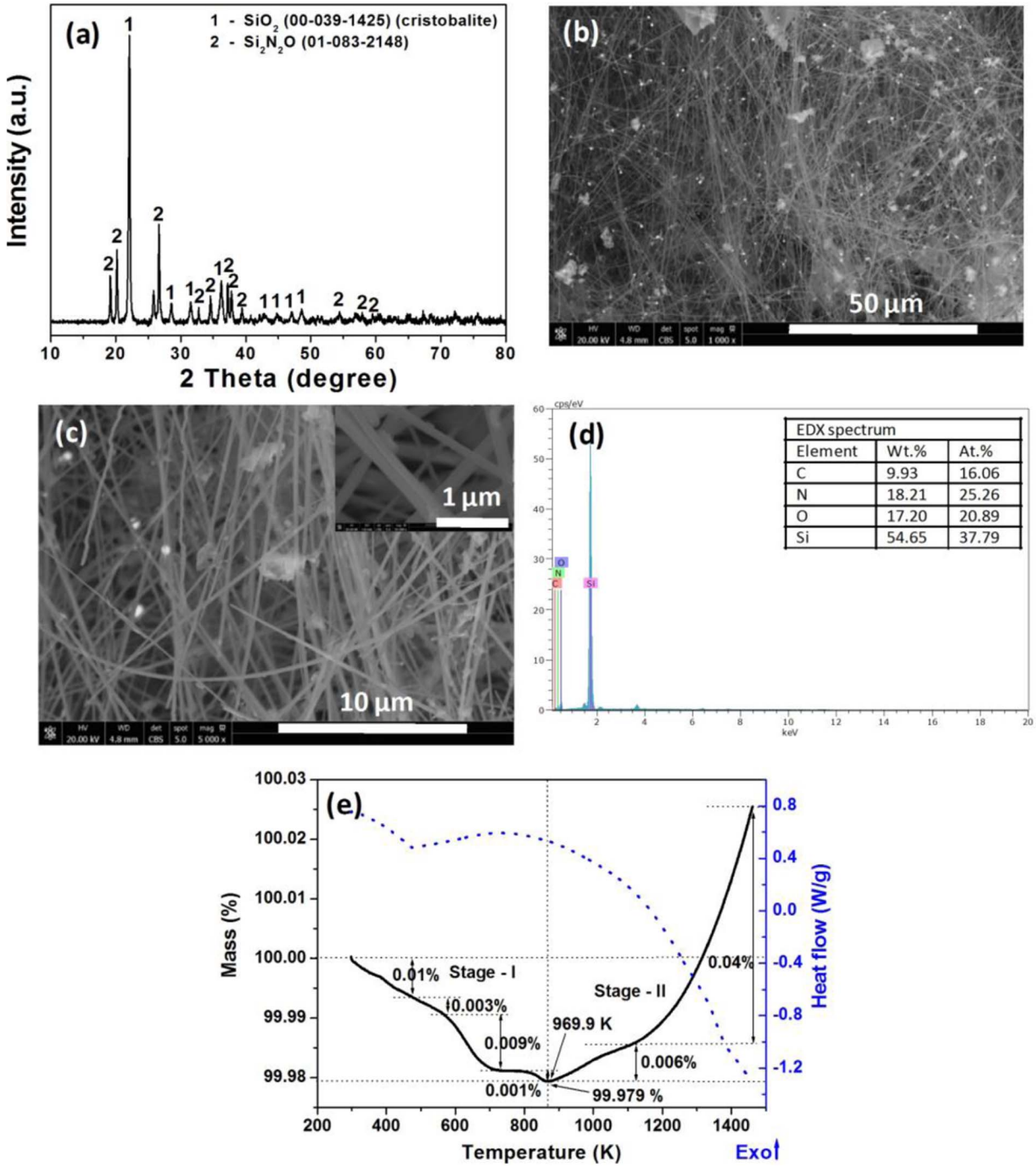

Figure 11. (a) XRD pattern of the Si_2N_2O/SiO_2 product obtained from SiO_2/graphite (molar ratio 1:1.5) by electro-deoxidation in $CaCl_2$ melt at 1173 K for 6 h at 2.8 V and subsequent heat-treatment in N_2 flow at 1473 K for 8 h. (b) SEM image and (c) high-resolution SEM image of the same sample with (d) corresponding EDX analysis. (e) TG/DSC curves of a 200 mg sample of SiC in N_2 flow of 100 mL/min at a scan rate of 20 K/min.

Acknowledgment

This study was partly funded through the Research Chair Grant Programme of The Research Council of the Sultanate of Oman.

Appendix: Stoichiometric Calculations on the Formation of Si_2N_2O from SiC

It is suggested that the formation of Si_2N_2O from SiC can progress via parallel reaction paths.

One reaction path is based on information from the literature concerning the mechanisms of active oxidation with residual oxygen and nitridation with gaseous N_2, as discussed in the main text, and can be expressed as follows.

$$\mathrm{SiC} + 2\,\mathrm{O}\ (\text{residual in SiC}) \rightarrow \mathrm{SiO}\ (g) + \mathrm{CO}\ (g) \qquad [A1]$$

$$2\,\mathrm{SiC} + \mathrm{CO}\ (g) + \mathrm{N_2}\ (g) \rightarrow \mathrm{Si_2N_2O} + 3\,\mathrm{C} \qquad [A2]$$

Each experiment involved 20 mg of electrochemically prepared SiC, with a residual oxygen content of 2.7 mass%. The mass of oxygen in the SiC was 0.54 mg, corresponding to 0.27 mg of oxygen present in the CO and the other half in the SiO. This would have allowed for the formation of 1.7 mg of Si_2N_2O.

It may alternatively be assumed that all the residual oxygen remained in the sample and that no SiO was released.

$$2\,SiC + O\ (\text{residual in SiC}) + N_2\,(g) \rightarrow Si_2N_2O + 2\,C \qquad [A3]$$

Now the mass of oxygen in the SiC of 0.54 mg would have allowed for the formation of 3.4 mg of Si_2N_2O.

Additional Si_2N_2O may have formed through the reaction with traces of O_2 and H_2O in the gas phase.

$$2\,SiC + {}^1\!/_2\,O_2\,(g) + N_2\,(g) \rightarrow Si_2N_2O + 2\,C \qquad [A4]$$

$$2\,SiC + H_2O\ (g) + N_2\,(g) \rightarrow Si_2N_2O + 2\,C + H_2\,(g) \qquad [A5]$$

The purity of the technical N_2 used in the nitridation experiments was specified as 99.999%, with 5 ppm of O_2 and 3 ppm of H_2O as the main impurities. With a flowrate of 100 mL/min over an exposure time of 16 h, including heating, dwelling and cooling, $2.0 \cdot 10^{-5}$ moles of O_2 and $1.2 \cdot 10^{-5}$ moles of H_2O passed through the reaction vessel, corresponding to a total mass of oxygen of 0.83 mg. This would have permitted the formation of 5.2 mg of Si_2N_2O.

A further source of oxygen may have been adsorbed O_2 and H_2O in the SiC reactant. This cannot be quantified, but may have been significant considering that the SiC was nanostructured and had a high specific surface area. Finally, some leakage of ambient air into the apparatus may have occurred, but this can again not be quantified.

Overall, the formation of milligram quantities of Si_2N_2O from the SiC is consistent with the experimental conditions applied in the nitridation experiments. The results therefore suggest that, by carefully determining the residual oxygen content in the SiC reactant and by carefully introducing further oxygen via the gas phase, the controlled synthesis of Si_2N_2O will become possible. An enhanced reaction rate should moreover be achievable by passing the gas stream through, rather than above, the SiC powder.

ORCID

D. Sri Maha Vishnu https://orcid.org/0000-0003-2487-5154
Jagadeesh Sure https://orcid.org/0000-0001-5041-9502
Carsten Schwandt https://orcid.org/0000-0002-6145-1230

References

1. H. Abderrazak and E. S. B. H. Hmida, "Silicon carbide: synthesis and properties," in: R. Gerhardt, (Ed.), *Properties and Applications of Silicon Carbide*, InTech, Croatia (2011), p. 361.
2. R. B. Wu, K. Zhou, C. Y. Yue, J. Wei, and Y. Pan, "Recent progress in synthesis, properties and potential applications of SiC nanomaterials," *Prog. Mater. Sci.*, **72**, 1 (2015).
3. G. C. T. Wei, "Beta SiC powders produced by carbothermic reduction of silica in a high-temperature rotary furnace," *J. Am. Ceram. Soc.*, **66**, C111 (1983).
4. N. Setaka and Z. Inoue, "Beta silicon carbide whiskers prepared on a molybdenum substrate," *J. Am. Ceram. Soc.*, **52**, 624 (1969).
5. N. Setaka and K. Ajiri, "Influence of vapor-phase composition on morphology of SiC single crystals," *J. Am. Ceram. Soc.*, **55**, 540 (1972).
6. J. Q. Hu, Q. Y. Lu, K. B. Tang, B. Deng, R. R. Jiang, Y. T. Qian, W. C. Yu, G. E. Zhou, X. M. Liu, and J. X. Wu, "Synthesis and characterization of SiC nanowires through a reduction-carburization route," *J. Phys. Chem. B*, **104**, 5251 (2000).
7. L. G. Ceballos-Mendivil, R. E. Cabanillas-López, J. C. Tánori-Córdova, R. Murrieta-Yescas, P. Zavala-Rivera, and J. H. Castorena González, "Synthesis and characterization of silicon carbide in the application of high temperature solar surface receptors," *Energy Procedia*, **57**, 533 (2014).
8. G. Z. Chen, D. J. Fray, and T. W. Farthing, "Direct electrochemical reduction of titanium dioxide to titanium in molten calcium chloride," *Nature*, **407**, 361 (2000).
9. D. J. Fray, "Novel methods for the production of titanium," *Int. Mater. Rev.*, **53**, 317 (2008).
10. K. S. Mohandas, "Direct electrochemical conversion of metal oxides to metal by molten salt electrolysis: a review," *Miner. Proc. Extract. Metall.*, **122**, 195 (2013).
11. D. J. Fray and C. Schwandt, "Aspects of the application of electrochemistry to the extraction of titanium and its applications," *Mater. Trans.*, **58**, 306 (2017).
12. X. Y. Yan, M. I. Pownceby, M. A. Cooksey, and M. R. Lanyon, "Preparation of TiC powders and coatings by electrodeoxidation of solid TiO_2 in molten salts," *Miner. Proc. Extract. Metall.*, **118**, 23 (2009).
13. J. H. Fan, Y. J. Yang, D. D. Tang, W. Xiao, X. H. Mao, and D. H. Wang, "Electrochemical synthesis of nano-metallic carbides from the mixtures of metal oxide and graphite," *J. Electrochem. Soc.*, **164**, E144 (2017).
14. L. Dai, X. Y. Wang, H. Z. Zhou, Y. Yu, J. Zhu, Y. H. Li, and L. Wang, "Direct electrochemical synthesis of zirconium carbide from zirconia/C precursors in molten calcium chloride," *Ceram. Inter.*, **41**, 4182 (2015).
15. A. M. Abdelkader and D. J. Fray, "Electrochemical synthesis of hafnium carbide powder in molten chloride bath and its densification," *J. Eur. Ceram. Soc.*, **32**, 4481 (2012).
16. X. C. Lang, H. W. Xie, Y. C. Zhai, and X. Y. Zhou, "Preparation and reaction mechanism of Cr_3C_2 by electrochemical reduction of the cathode self-sintered in molten $CaCl_2$ salt," *Rare Metal Mater. Eng.*, **42**, 1926 (2013).
17. L. Dai, Y. Lu, X. Y. Wang, J. Zhu, Y. H. Li, and L. Wang, "Production of nano-sized chromium carbide powders from Cr_2O_3/C precursors by direct electrochemical reduction in molten calcium chloride," *Int. J. Refract. Met. Hard Mater.*, **51**, 153 (2015).
18. Q. S. Song, Q. Xu, J. C. Meng, T. P. Lou, Z. Q. Ning, Y. Qi, and K. Yu, "Preparation of niobium carbide powder by electrochemical reduction in molten salt," *J. Alloys Compd.*, **647**, 245 (2015).
19. D. H. Tran-Nguyen, D. Jewell, and D. J. Fray, "Electrochemical preparation of tungsten, tungsten carbide and cemented tungsten carbide," *Miner. Proc. Extract. Metall.*, **123**, 53 (2014).
20. C.-R. Zhao, J.-Y. Yang, and S.-G. Lu, "Preparation of SiC nanowires by direct electro-reduction of SiO_2/C pellets in molten salt," *Chin. J. Inorg. Chem.*, **29**, 2543 (2013).
21. X. L. Zou K. Zheng, X. G. Lu, Q. Xu, and Z. F. Zhou, "Solid oxide membrane-assisted controllable electrolytic fabrication of metal carbides in molten salt," *Faraday Discuss.*, **190**, 53 (2016).
22. X. L. Zou, L. Ji, X. G. Lu, and Z. F. Zhou, "Facile electrosynthesis of silicon carbide nanowires from silica/carbon precursors in molten salt," *Sci. Rep.*, **7**, 9978 (2017).
23. X. L. Zou, L. Ji, H. Y. Hsu, K. Zheng, Z. Y. Pang, and X. G. Lu, "Designed synthesis of SiC nanowire-derived carbon with dual-scale nanostructures for supercapacitor applications," *J. Mater. Chem. A*, **6**, 12724 (2018).
24. A. Roine, *HSC Chemistry*, Version 5.1, Outokumpu Research Oy, Pori, Finland, 2002.
25. X. B. Jin, P. Gao, D. H. Wang, X. H. Hu, and G. Z. Chen, "Electrochemical preparation of silicon and its alloys from solid oxides in molten calcium chloride," *Angew. Chem. Int. Ed.*, **43**, 733 (2004).
26. W. Xiao, X. B. Jin, Y. Deng, D. H. Wang, X. H. Hu, and G. Z. Chen, "Electrochemically driven three-phase interlines into insulator compounds: electroreduction of solid SiO_2 in molten $CaCl_2$," *Chem. Phys. Chem.*, **7**, 1750 (2006).
27. J. J. Peng, N. Q. Chen, R. He, Z. Y. Wang, S. Dai, and X. B. Jin, "Electrochemically driven transformation of amorphous carbons to crystalline graphite nanoflakes: a facile and mild graphitization method," *Angew. Chem. Int. Ed.*, **56**, 1751 (2017).
28. L. Ceja-Cárdenas and J. Lemus-Ruiz, *Silicon Nitride: A Review of Recent Research*, Nova Science Publishers, NY (2014).
29. D. Sri Maha Vishnu, N. Sanil, L. Shakila, G. Panneerselvam, R. Sudha, K. S. Mohandas, and K. Nagarajan, "A study of the reaction pathways during electrochemical reduction of dense Nb_2O_5 pellets in molten $CaCl_2$ medium," *Electrochim. Acta*, **100**, 51 (2013).
30. C. Schwandt and D. J. Fray, "The electrochemical reduction of chromium sesquioxide in molten calcium chloride under cathodic potential control," *Z. Naturforsch. A*, **62**, 655 (2007).
31. P. A. Kistler-De Coppi and W. Richarz, "Phase transformations and grain growth in silicon carbide powders," *Int. J. High Technol. Ceram.*, **2**, 99 (1986).
32. T. Nohira, K Yasuda, and Y. Ito, "Pinpoint and bulk electrochemical reduction of insulating silicon dioxide to silicon," *Nat. Mater.*, **2**, 397 (2003).
33. G. M. Li, D. H. Wang, and Z. Chen, "Direct reduction of solid Fe_2O_3 in molten $CaCl_2$ by potentially green process," *J. Mater. Sci. Technol.*, **25**, 767 (2009).
34. D. Sri Maha Vishnu, N. Sanil, G. Panneerselvam, R. Sudha, K. S. Mohandas, and K. Nagarajan, "Mechanism of direct electrochemical reduction of solid UO_2 to uranium metal in $CaCl_2$-48mol% NaCl melt," *J. Electrochem. Soc.*, **160**, D394 (2013).
35. D. Sri Maha Vishnu, N. Sanil, and K. S. Mohandas, "Difference in the mechanism of electrochemical deoxidation of conducting and non-conducting solid oxide preforms: an experimental demonstration with TiO_2 and SiO_2 pellet electrodes in $CaCl_2$ melt," *Res. Rev. J. Mater. Sci.*, **5**, 193 (2017).
36. C. Schwandt and D. J. Fray, "Determination of the kinetic pathway in the electrochemical reduction of titanium dioxide in molten calcium chloride," *Electrochim. Acta*, **51**, 66 (2005).
37. T. Wu, X. B. Jin, W. Xiao, X. H. Hu, D. H. Wang, and G. Z. Chen, "Thin pellets: fast electrochemical preparation of capacitor tantalum powders," *Chem. Mater.*, **19**, 153 (2007).
38. W. Xiao, X. Wang, H. Y. Yin, H. Zhu, X. H. Mao, and D. H. Wang, "Verification and implications of the dissolution-electrodeposition process during the electro-reduction of solid silica in molten $CaCl_2$," *RSC Advances*, **2**, 7588 (2012).
39. I. Yu. Tishchenko, O. O. Ilchenko, and P. O. Kuzema, "TGA-DSC-MS analysis of silicon carbide and of its carbon-silica precursor," *Chem. Phys. Technol. Surf.*, **6**, 216 (2015).
40. J. Roy, S. Chandra, S. Das, and S. Maitra, "Oxidation behavior of silicon carbide – a review," *Rev. Adv. Mater. Sci.*, **38**, 29 (2014).
41. R. G. Munro and S. J. Dapkunas, "Corrosion characteristics of silicon carbide and silicon nitride," *J. Res. Natl. Inst. Stand. Technol.*, **98**, 607 (1993).